

## New insight about the effective restoration of $U_A(1)$ symmetry

Xiang Li,<sup>1,2</sup> Wei-jie Fu,<sup>3</sup> and Yu-xin Liu<sup>1,2,4,\*</sup>

<sup>1</sup>*Department of Physics and State Key Laboratory of Nuclear Physics and Technology, Peking University, Beijing 100871, China*

<sup>2</sup>*Collaborative Innovation Center of Quantum Matter, Beijing 100871, China*

<sup>3</sup>*School of Physics, Dalian University of Technology, Dalian 116024, China*

<sup>4</sup>*Center for High Energy Physics, Peking University, Beijing 100871, China*



(Received 24 October 2019; revised manuscript received 23 January 2020; accepted 31 January 2020; published 26 March 2020)

The effective restoration of the  $U_A(1)$  symmetry is revisited by implementing the functional renormalization group approach combined with the 2 + 1 flavor Polyakov-loop quark-meson model. A temperature-dependent 't Hooft term is taken to imitate the restoration of the  $U_A(1)$  symmetry. Order parameters, meson spectrum and mixing angles, especially the pressure, the entropy density, and the speed of sound of the system are calculated to explore the effects of different  $U_A(1)$  symmetry restoration patterns. We show then that the temperature for the restoration of the  $U_A(1)$  symmetry is much higher than that for the chiral symmetry  $SU_A(3)$ .

DOI: [10.1103/PhysRevD.101.054034](https://doi.org/10.1103/PhysRevD.101.054034)

### I. INTRODUCTION

Studies on the strong interaction system (QCD system) have been attractive over decades, since a full understanding of the QCD system is crucial for exploring the fundamental structure of nature. Due to the nonperturbative character and special vacuum structure of QCD, many problems of the QCD system remain unsettled; for instance, the  $U_A(1)$  anomaly and its restoration is a long-standing one in this area [1–7].

In the QCD system, the spontaneous breaking of the chiral symmetry  $SU_A(3)$  leads to eight pseudo-Goldstone bosons. The left axial symmetry  $U_A(1)$  is violated by a quantum anomaly and results in a heavy meson, i.e.,  $\eta'$  [2]. However, it is predicted in Ref. [3] that  $U_A(1)$  symmetry can be effectively restored at a high temperature due to the suppression of the instanton density of the QCD vacuum. This prediction is proved later in many lattice QCD simulation results [8–12], whereas the specific temperature for  $U_A(1)$  to be restored is still far from clear and requires more investigations.

Depending on whether the  $U_A(1)$  symmetry is restored before the chiral phase transition, the universal class of the whole system will be different, and the order of the chiral phase transition can be changed, this leads then to different

Columbia plots [4,5]. Various quantities (such as the topological susceptibility and the mesonic correlators [8–12]) have been calculated in lattice QCD to investigate the restoration of the  $U_A(1)$  symmetry. The calculated topological susceptibility and the mass splitting between the scalar and pseudoscalar mesons (for example,  $a_0$  and  $\pi$ ) all tend to decrease near the chiral phase transition. These results indicate a partial restoration of the  $U_A(1)$  symmetry near the chiral phase transition, but more numerical efforts are needed to reach a definite conclusion.

Besides the lattice QCD method, continuum field approaches such as the Dyson-Schwinger equation approach and the functional renormalization group approach have also been taken to survey the  $U_A(1)$  problem (see, e.g., Refs. [13–16]). Compared with the lattice QCD method, the continuum field approach usually requires less numerical efforts, and the chiral symmetry can be implemented easily.

In addition to the first principle approach mentioned above,  $U_A(1)$  symmetry has also been investigated via effective models (see, e.g., Refs. [17–35]). Simple phenomenological models (for example, the linear sigma model, the Nambu–Jona–Lasino model, and the quark-meson model) are taken to approximate the QCD approach and the  $U_A(1)$  anomaly is usually implemented via the 't Hooft term [1]. It is shown that the order parameter and meson spectrum will be significantly affected when the effective restoration of the  $U_A(1)$  symmetry is considered, and several efficient signals have been predicted in heavy ion collision experiments to detect the  $U_A(1)$  restoration effect (see, e.g., Ref. [17]). And it has also been shown in Ref. [19] that the  $U_A(1)$  symmetry remains broken when the chiral transition happens, but this prediction is somehow model dependent, and more detailed investigation is still needed.

\*yxliu@pku.edu.cn

Published by the American Physical Society under the terms of the [Creative Commons Attribution 4.0 International license](https://creativecommons.org/licenses/by/4.0/). Further distribution of this work must maintain attribution to the author(s) and the published article's title, journal citation, and DOI. Funded by SCOAP<sup>3</sup>.

In this work, we employ the functional renormalization group (FRG) approach [33–45] combined with the 2 + 1 flavor Polyakov-loop quark-meson model [45–49] (PQM) to investigate the  $U_A(1)$  problem, and there have already been some proceeding works using a similar FRG approach (see, e.g., Refs. [33–35,50]). It is well known that the PQM model is an effective approximation of QCD in the low energy region, and the FRG approach can go beyond the widely used mean-field approximation. The effective restoration of the  $U_A(1)$  symmetry is imitated via a temperature-dependent 't Hooft term deduced from lattice QCD simulations and theoretical derivations [17,20,51]. With such a temperature-dependent 't Hooft term, order parameters, the meson spectrum, mixing angles, pressure, entropy density, and speed of sound of the system are calculated to explore the response of the system to the restoring  $U_A(1)$  symmetry. Compared with previous works, the restoration of the  $U_A(1)$  symmetry is viewed from a new perspective: thermodynamical quantities of the system are taken to identify the effect of the  $U_A(1)$  symmetry restoration. As we will see, an unphysical thermodynamical result will appear if the  $U_A(1)$  symmetry is restored before the chiral phase transition. We show then that the  $U_A(1)$  symmetry is still broken as the chiral phase transition happens.

The remainder of this paper is organized as follows. In Sec. II, we introduce briefly the main aspects of the FRG approach and the PQM model. Some discussions about the temperature-dependent 't Hooft term are also given. In Sec. III, we show the obtained results and discuss the underlying mechanism. In Sec. IV, we give our summary and some remarks.

## II. THEORETICAL FRAMEWORK

In this section, we describe concisely the FRG approach and the PQM model for self-consistency, and more details can be found in Refs. [34,35,48,49,52,53]. Briefly speaking, the PQM model can be recognized as a linear sigma model coupled with a static gluon background field, with the gluon field being integrated out. Its Lagrangian reads simply

$$\begin{aligned} \mathcal{L} = & \bar{\psi}(\not{\partial} - i\gamma_4 A_4 + g\Sigma_5)\psi + \text{Tr}[\partial_\mu \Sigma \cdot (\partial_\mu \Sigma)^\dagger] \\ & + U(\Sigma) - h_x \sigma_x - h_y \sigma_y - c_a \xi + V_{\text{poly}}(\Phi), \end{aligned} \quad (1)$$

where  $\psi$  represents the three flavor (u,d,s) quark field, and  $\Sigma = (\sigma_a + i\pi_a)T^a$  is a matrix which contains scalar and pseudoscalar meson nonets. The  $\sigma_x$  and  $\sigma_y$  are related to the meson fields via a rotation, which read

$$\begin{pmatrix} \sigma_x \\ \sigma_y \end{pmatrix} = \frac{1}{\sqrt{3}} \begin{pmatrix} 1 & \sqrt{2} \\ -\sqrt{2} & 1 \end{pmatrix} \begin{pmatrix} \sigma_8 \\ \sigma_0 \end{pmatrix}, \quad (2)$$

where the subscripts  $x, y$  simply denote two directions in meson field space (see, e.g., Ref. [52]). Since the  $\sigma_x, \sigma_y$  is

related to the light and strange quark condensate, respectively, the terms  $h_x \sigma_x$  and  $h_y \sigma_y$  then break the  $SU_V(3) \times SU_A(3)$  symmetry explicitly. The  $V_{\text{poly}}$  is a phenomenological potential of the Polyakov-loop  $\Phi$ , which is added to imitate the confinement effect. For the specific definition of other terms in Eq. (1), see Refs. [52,53].

Among all the terms in Eq. (1), the 't Hooft term  $c_a \xi$  is quite special:  $\xi = \det(\Sigma) + \det(\Sigma^\dagger)$  breaks the  $U_A(1)$  symmetry explicitly, and the  $c_a$  is a parameter measuring the strength of the axial anomaly. This term originates from the nontrivial vacuum structure of the gauge field, which can be characterized by the so-called winding numbers. The topologically different vacuums can be linked by an instanton, which is also the Gaussian stable point of the path integral and should contribute to the partition function. However, the  $U_A(1)$  charge of quarks is not conserved in an instanton background and thus, leads to the effective  $U_A(1)$  breaking term  $c_a \xi$  [1,6].

When the temperature effect is considered, the contribution from the instantons will get suppressed by Debye screening, and the  $U_A(1)$  symmetry can be effectively restored [3]. In order to take the restoration of the  $U_A(1)$  symmetry into consideration, it is usual to parametrize the  $c_a$  as a function of temperature [17,20,51]. Lattice QCD simulations show that the topological susceptibility is nearly unchanged at low temperature [8], and theoretical derivations predict an exponential decay of the instanton density at high temperature [3]. Combining these two aspects, we employ the form proposed in Ref. [51], which reads

$$c_a(T) = \begin{cases} c_a(0), & T < T_r; \\ c_a(0) \exp\left[-\frac{(T-T_r)^2}{b^2}\right], & T > T_r; \end{cases} \quad (3)$$

where  $c_a(0)$  is a constant obtained by fitting a meson spectrum at vacuum.  $T_r$  and  $b$  are two free parameters:  $T_r$  is simply the starting temperature for the  $U_A(1)$  symmetry to be restored and  $b$  determines the restoration speed. In this work, we will mainly tune the  $T_r$  to control the restoration pattern of the  $U_A(1)$  symmetry. Note that there exist other ways to parametrize the  $c_a$  (see, e.g., Refs. [17,20]), but they are all similar with each other and would not make much difference to the results.

It is worth mentioning that the  $c_a$  will receive contributions from thermal fluctuations and then acquire a temperature dependence even without the instanton effect (see, e.g., Refs. [50,54,55]). So Eq. (3) can be seen as a crude approximation of  $U_A(1)$  restoration, which considers instanton effect only and neglects thermal fluctuation contributions.

After introducing the Lagrangian, the FRG approach can be employed to study the thermodynamics of the PQM system. A functional evolution equation for the effective action  $\Gamma_k$  is derived to integrate different momentum shell out gradually [36], which reads

$$\partial_k \Gamma_k = \frac{1}{2} \text{Tr} \left[ \frac{\partial_k R_k^B}{\Gamma_k^{2B} + R_k^B} \right] - \text{Tr} \left[ \frac{\partial_k R_k^F}{\Gamma_k^{2F} + R_k^F} \right], \quad (4)$$

where  $R_k^{B,F}$  are the momentum-dependent mass terms assigned to the quarks and mesons, and  $\Gamma_k^{2B}, \Gamma_k^{2F}$  denote the second derivatives of  $\Gamma_k$  with respect to the corresponding fields. Compared with the traditional mean-field approximation, the FRG approach incorporates meson fluctuations into the evolution. It is well known that mesons such as pions dominate at low temperature and their fluctuations affect the system significantly (see, e.g., Refs. [52,53]). Thus, the FRG approach is usually known to be a method beyond the mean-field approximation.

It is usually impossible to solve Eq. (4) exactly, we take then the local potential approximation (LPA) in this paper to simplify the problem. The truncated  $\Gamma_k$  reads

$$\Gamma_k = \int d^4x \bar{\psi} (\not{\partial} - i\gamma_4 A_4 + g\Sigma_5) \psi + \text{Tr} [\partial_\mu \Sigma \cdot (\partial_\mu \Sigma)^\dagger] + U_k(\rho_1, \rho_2) - h_x \sigma_x - h_y \sigma_y - c_a \xi + V_{\text{poly}}(\Phi), \quad (5)$$

where  $U_k$  is the only flowing term and contains two  $U_V(3) \times U_A(3)$  invariants  $\rho_1, \rho_2$ , which read explicitly

$$\begin{aligned} \rho_1 &= \text{Tr} [\Sigma \cdot \Sigma^\dagger], \\ \rho_2 &= \text{Tr} \left[ \left( \Sigma \cdot \Sigma^\dagger - \frac{1}{3} \rho_1 \right)^2 \right]. \end{aligned} \quad (6)$$

We can then substitute Eq. (5) into Eq. (4) and obtain the flow equation for  $U_k$  as

$$\begin{aligned} \partial_k U_k &= \frac{k^4}{12\pi^2} \left\{ \sum_b \frac{1}{E_b} [1 + 2n_b(E_b)] \right. \\ &\quad \left. - \sum_{f=u,d,s} \frac{4N_c}{E_f} [1 - 2\tilde{n}_f(E_f, \Phi)] \right\}, \end{aligned} \quad (7)$$

where  $E_i = \sqrt{k^2 + m_i^2}$  and the quark masses read

$$m_{u,d} = \frac{g}{2} \sigma_x, \quad m_s = \frac{g}{\sqrt{2}} \sigma_y. \quad (8)$$

Meson masses  $m_b$  are given by the eigenvalues of the Hessian matrix  $H_{i,j}$ , which reads

$$H_{i,j} = \frac{\partial^2 U_k}{\partial \sigma_i \partial \sigma_j}. \quad (9)$$

The specific form of the meson masses are quite tedious and can be found in Refs. [33,52].  $n_b$  is the ordinary boson distribution function while  $\tilde{n}_f$  denotes the Polyakov-loop modified fermion distribution function, which reads

$$\tilde{n}_f(E_f, \Phi) = \frac{1 + 2\Phi e^{\beta E_f} + \Phi e^{2\beta E_f}}{1 + 3\Phi e^{\beta E_f} + 3\Phi e^{2\beta E_f} + e^{3\beta E_f}}. \quad (10)$$

Note that  $U_k(\rho_1, \rho_2)$  will develop a dependence on  $\Phi$  via the quark's fluctuations in the last line of Eq. (7). To accomplish the calculation, we adopt the three-dimensional infrared regulators proposed in Refs. [37–42]. This flow equation can be solved numerically by the Taylor method [34,35,48,49,52,53], and the parameters used in this work are the same as those in Ref. [53]. We can then get the thermodynamic property of the PQM system after the full  $U_0(\Sigma, \Phi)$  is obtained.

### III. RESULT

After Eq. (7) is solved, various quantities can be obtained via the effective potential  $\tilde{U}(\sigma_x, \sigma_y, \Phi)$ , which reads

$$\begin{aligned} \tilde{U}(\sigma_x, \sigma_y, \Phi) &= U_0(\sigma_x, \sigma_y, \Phi) + V_{\text{poly}}(\Phi) \\ &\quad - h_x \sigma_x - h_y \sigma_y - c_a \frac{\sigma_x^2 \sigma_y}{2\sqrt{2}}. \end{aligned} \quad (11)$$

Note that the 't Hooft term  $c_a \xi$  has been reduced to the last term in Eq. (11) since only the  $\sigma_x$  and  $\sigma_y$  remain nonzero now. The quantities  $\tilde{\sigma}_x$  and  $\tilde{\Phi}$  corresponding to the minimums of the effective potential  $\tilde{U}$  are usually taken as the order parameters for the chiral and the deconfinement phase transition, respectively. And the chiral pseudocritical temperature  $T_c^\chi$  extracted from the inflection point of  $\tilde{\sigma}_x$  is  $T_c^\chi = 208$  MeV if the anomaly strength  $c_a$  keeps constant.

In order to investigate the effects of different  $U_A(1)$  symmetry restoration patterns, we set the  $U_A(1)$  restoration temperature  $T_r$  to three typical values 150, 200, and 250 MeV. Another parameter  $b$  is set to 50 MeV, and different choices of the  $b$  would not induce much difference.

#### A. Order parameters

The calculated order parameters are displayed in Figs. 1 and 2. As we see directly from the Fig. 1, the  $\tilde{\sigma}_x$  decreases monotonously with the rising of temperature. This simply means that the chiral symmetry  $SU_A(3)$  is getting restored gradually. After the restoration of  $U_A(1)$  symmetry is considered,  $\tilde{\sigma}_x$  will get reduced significantly compared with the constant  $c_a$  case, and the chiral pseudocritical temperature is then shifted to a lower value: the  $T_c^\chi$  for  $T_r = 150$  MeV case is lowered to 177 MeV, while the  $T_c^\chi$  for  $T_r = 200, 250$  MeV cases is nearly unchanged compared with the constant  $c_a$  case. These effects of  $U_A(1)$  restoration are also predicted in Refs. [17,20,51] and can be explained via Eq. (11) as: the 't Hooft term  $c_a \xi$  acts as a negative cubic term in the effective potential  $\tilde{U}(\sigma_x, \sigma_y, \Phi)$ , thus a decreasing 't Hooft term will definitely accelerate the reduction of the order parameter. And at high temperature

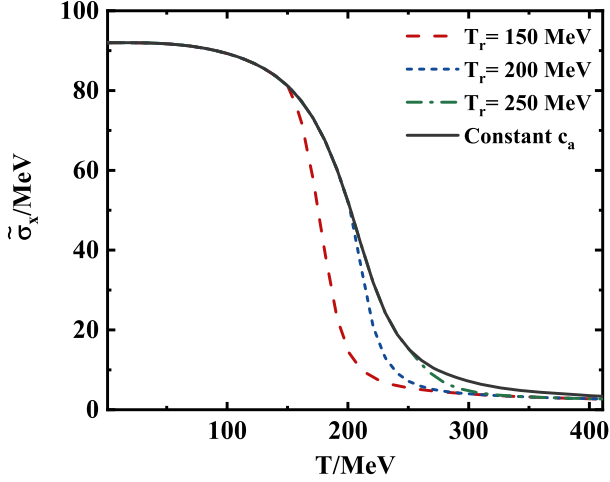


FIG. 1. Calculated  $\tilde{\sigma}_x$  as functions of temperature at several values of  $T_r$ .

region, the chiral symmetry has been recovered; thus, the effect of the 't Hooft term becomes negligible. As for the deconfinement phase transition, the calculated order parameter  $\tilde{\Phi}$  shown in Fig. 2 displays their own similar behaviors:  $\tilde{\Phi}$  increases and then the deconfinement phase transition is triggered earlier as the  $U_A(1)$  restoration is considered, while the variation amplitudes of  $\tilde{\Phi}$  are much smaller than the  $\tilde{\sigma}_x$ .

### B. Meson spectrum and meson mixing

The same effect of the  $U_A(1)$  symmetry restoration is also manifested in meson spectrum. It is well known that the  $\sigma$  and  $\pi$  mesons form a four-dimensional representation of the  $SU_V(2) \times SU_A(2)$  group and they will get degenerate when the chiral symmetry is restored. Figure 3 shows evidence that the degeneration of the  $\sigma$  and  $\pi$  is also facilitated by the  $U_A(1)$  symmetry restoration effect, which

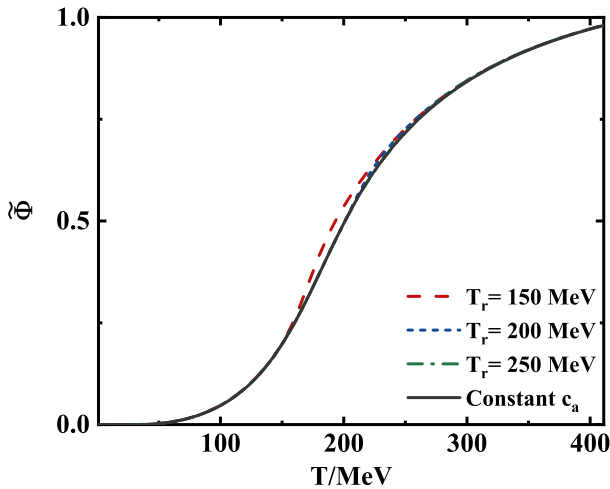


FIG. 2. Calculated Polyakov loop  $\tilde{\Phi}$  as functions of temperature at several values of  $T_r$ .

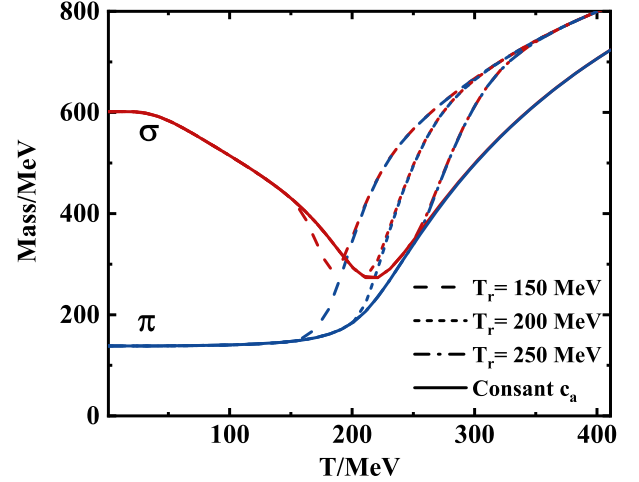


FIG. 3. Calculated masses of  $\pi$  and  $\sigma$  mesons as functions of temperature at several values of  $T_r$ .

is consistent with the behaviors of order parameters displayed in Figs. 1 and 2.

A meson spectrum can also be implemented to explore the status of the  $U_A(1)$  symmetry. Figure 4 shows the calculated spectrum of  $a_0$  and  $\pi$  meson; these two mesons have the same quantum number except for parity, and they only get degenerate when axial symmetry is restored. As we can see from Fig. 4, when the 't Hooft term keeps constant, there is always a mass splitting  $\Delta m^2$  between  $\pi$  and  $a_0$  which reads [33,52]

$$\Delta m^2 = m_{a_0}^2 - m_\pi^2 = \frac{\partial U_0}{\partial \rho_2} \tilde{\sigma}_x^2 + \sqrt{2} c_a \tilde{\sigma}_y. \quad (12)$$

The first term in Eq. (12) originates from the chiral symmetry breaking while the second term is due to the  $U_A(1)$  anomaly, so that axial symmetry is broken at any temperature as long as  $c_a$  is kept finite [4,17]. After the

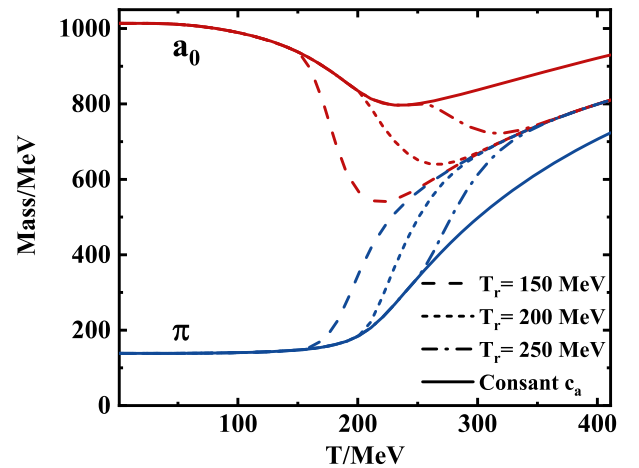


FIG. 4. Calculated masses of  $\pi$  and  $a_0$  mesons as functions of temperature at several values of  $T_r$ .

anomaly strength  $c_a$  acquires a temperature dependence as Eq. (3),  $\Delta m^2$  begins to decrease.  $\pi$  will grow heavy gradually and finally get degenerate with  $a_0$ ;  $U_A(1)$  symmetry is then restored. Comparing the results shown in Figs. 3 and 4, we can notice that the degeneration temperature of  $(a_0, \pi)$  is always much higher than the one corresponding to the chiral partners, the  $(\sigma, \pi)$  multiplet, which is consistent with the lattice QCD simulations [9]. Hence, we deduce that the  $U_A(1)$  symmetry is still broken as the chiral symmetry is restored. The same conclusion can be drawn from a different perspective in the following Sec. III C.

When chiral symmetry  $SU_A(3)$  is explicitly broken, the particles that belong to different representations of the symmetry group can get mixed with each other and forms the mass eigenstate. For example, (pseudo)scalar mesons in the meson matrix  $\Sigma$  will get rotated to form physical particles, which reads

$$\begin{pmatrix} \eta \\ \eta' \end{pmatrix} = \begin{pmatrix} \cos \theta_p & -\sin \theta_p \\ \sin \theta_p & \cos \theta_p \end{pmatrix} \begin{pmatrix} \pi_8 \\ \pi_0 \end{pmatrix},$$

$$\begin{pmatrix} f_0 \\ \sigma \end{pmatrix} = \begin{pmatrix} \cos \theta_s & -\sin \theta_s \\ \sin \theta_s & \cos \theta_s \end{pmatrix} \begin{pmatrix} \sigma_8 \\ \sigma_0 \end{pmatrix}. \quad (13)$$

These mixing angles  $\theta_p$  and  $\theta_s$  are very sensitive to the status of  $U_A(1)$  symmetry [18] and can be calculated to study the effect of  $U_A(1)$  restoration. The expressions for  $\theta_{p,s}$  reads simply

$$\tan(2\theta_i) = \frac{2(m_i^2)_{0,8}}{(m_i^2)_{0,0} - (m_i^2)_{8,8}} \quad (i = s, p), \quad (14)$$

where  $m_i^2$  with subscripts are the second derivatives of  $U_0$  with respect to the corresponding fields. We can see from Eq. (14) that  $\theta_i$  is actually a multivalued function with a period  $\pi/2$ . The branch cut of  $\theta_i$  will be chosen at each temperature point to ensure that the masses of the mesons are continuous with the increasing of temperature. We would like to mention here that the branch cut for  $\theta_p$  is fixed to  $[-\pi/4, \pi/4]$  in Ref. [51], and this choice of the branch cut results in discontinuous masses of the  $\eta$  and  $\eta'$  as functions of temperature. However, since the chiral phase transition with physical quark masses at zero density is well known as a crossover, we think that the discontinuous behavior of the masses should be avoided by choosing the branch cut for  $\theta_p$  carefully.

The calculated mixing angles with a constant 't Hooft term are shown in Fig. 5. As we can see clearly,  $\theta_p$  and  $\theta_s$  will both increase and approach the ideal mixing angle  $35^\circ$  with the ascending of temperature. When the ideal mixing angle  $35^\circ$  is reached,  $\eta'$  and  $\sigma$  will only contain light  $u$ -,  $d$ -(anti)quarks while the  $\eta$  and  $f_0$  contain only  $s$  (anti) quarks according to the relation in Eq. (13), which is consistent with the results in Refs. [18,21]. After the  $U_A(1)$  restoration effect is considered, the pseudoscalar mixing

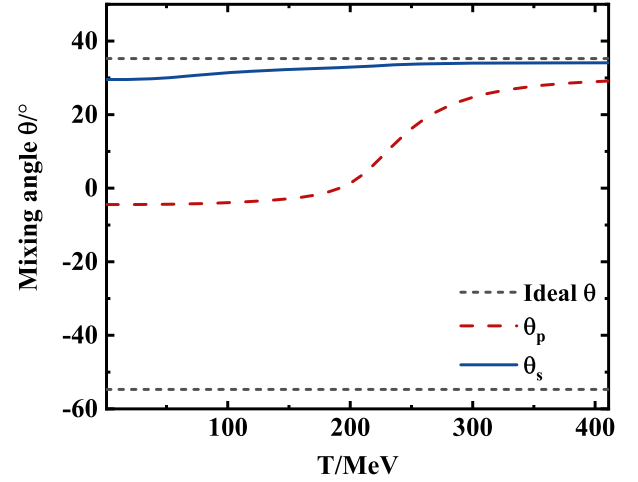


FIG. 5. Calculated mixing angles  $\theta_p$ ,  $\theta_s$  as functions of temperature with a constant 't Hooft term.

angle  $\theta_p$  will be changed significantly as displayed in Fig. 6. It is evident that the  $\theta_p$  will decrease to approach another ideal mixing angle  $-55^\circ$  at high temperature; this simply means  $\eta'$  will become almost strange instead at high temperature while  $\eta$  will become nonstrange, which is the same as the results given in Refs. [20]. And this result is consistent with the calculated spectrum of  $\eta$ ,  $\eta'$ , and  $a_0$  mesons displayed in Figs. 7 and 8: the chiral partner of  $a_0$  is changed from  $\eta'$  to  $\eta$  after the  $U_A(1)$  restoration at high temperature is considered, which means that the quark content of the  $\eta$ ,  $\eta'$  has been interchanged.

Before we close this subsection, we would like to compare our results with the previous works which calculate the  $\eta$ - $\eta'$  mixing angles and the mass spectrum with different approaches and truncations [34,50,51,56].

For example, Ref. [34] employs the FRG approach combined with the quark-meson model to study the  $\eta$ - $\eta'$

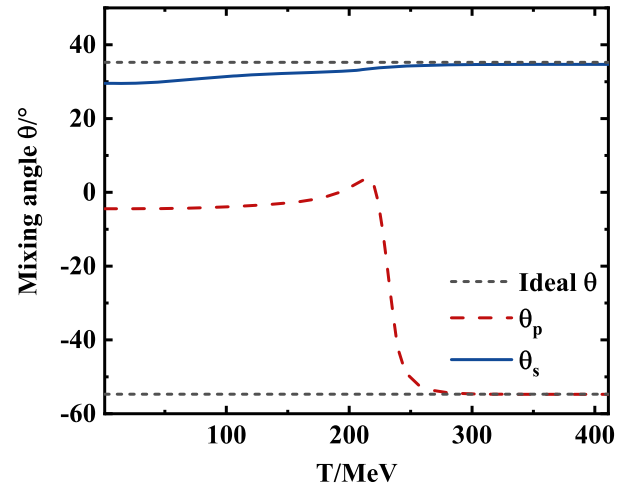


FIG. 6. Calculated mixing angles  $\theta_p$ ,  $\theta_s$  as functions of temperature with a decreasing 't Hooft term.  $T_r$  is chosen to be 200 MeV.

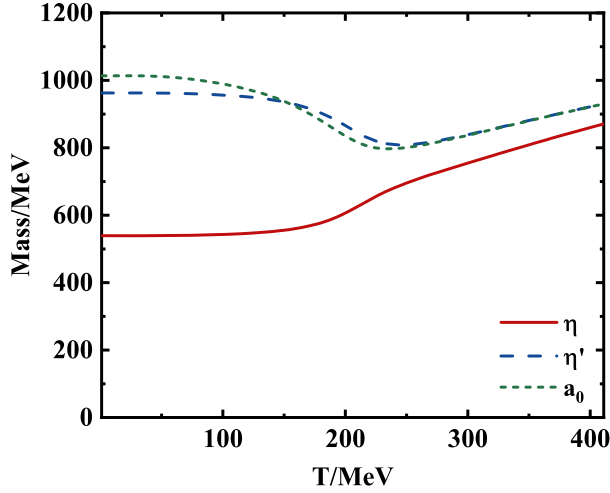


FIG. 7. Calculated masses of  $\eta$ ,  $\eta'$ , and  $a_0$  mesons with a constant 't Hooft term.

mixing problem. However, it makes use of a constant 't Hooft term and goes beyond the LPA approximation by taking the flow of anomalous dimensions and Yukawa coupling into considerations. It shows that the  $\theta_p$  will approach  $-55^\circ$  instead at a high temperature, which differs from our LPA result shown in Fig. 5. And instead of a constant 't Hooft term, a nontrivial structure of a 't Hooft term as a function of an order parameter and temperature is considered in Ref. [50]. Meson fluctuations are taken into considerations by the FRG approach, and they will strengthen the  $U_A(1)$  anomaly. Thus, no drop in the  $\eta'$  mass around  $T_c^x$  is observed compared with the  $\eta'$  mass shown in Figs. 7 and 8.

Moreover, the  $U_A(1)$  problem has also been studied in mean-field approximation. The same PQM model and temperature-dependent 't Hooft term as declared in Eqs. (1) and (3) are employed in Ref. [51]. Their results are similar with ours except they choose a different branch cut for  $\theta_p$  and results in discontinuous  $\eta, \eta'$  masses as mentioned below Eq. (14). However, after the effects of the (axial-)vector mesons are considered, the  $\theta_p$  will be significantly affected [56]. It is shown in Ref. [56] that the  $\theta_p$  will be driven to  $-55^\circ$  at a high temperature with a constant 't Hooft term due to the vector meson effect, which differs from the  $\theta_p$  behaviors plotted in Fig. 5.

We can see from the above discussions that the  $\eta$ - $\eta'$  mixing angle and their spectrum are highly sensitive to many other effects except the instanton effect discussed in our work. And in order to survey the  $\eta$ - $\eta'$  mixing problem more thoroughly, we need to take all the effects discussed above into considerations.

### C. Thermodynamical quantity

Besides order parameters and meson spectrum, thermodynamical quantities such as pressure can also be calculated to manifest how the system responds to the  $U_A(1)$

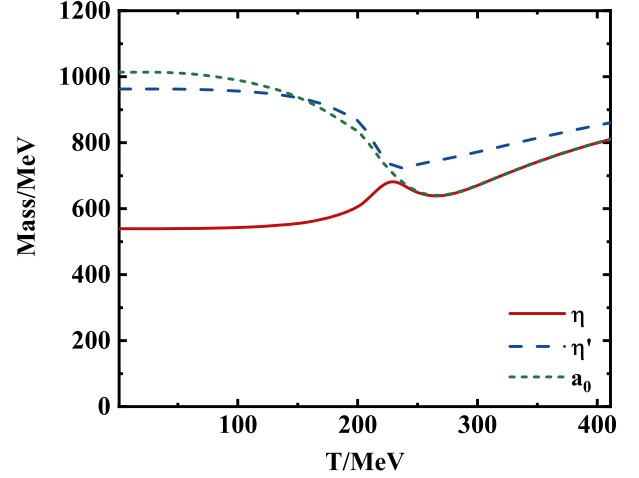


FIG. 8. Calculated masses of  $\eta$ ,  $\eta'$ , and  $a_0$  mesons with a decreasing 't Hooft term.  $T_r$  is chosen to be 200 MeV.

restoration. The calculated normalized pressure is displayed in Fig. 9. The most striking aspect we obtained is that the pressure becomes negative in the chiral transition region if the 't Hooft term begins to drop down too early. And the  $U_A(1)$  symmetry restoration continues to reduce the pressure at any certain temperature until the temperature is high enough, only then the pressure differences between different restoration patterns become negligible. This unnatural behavior of the pressure is not seen in previous lattice QCD simulations [57,58] and can be explained via Eq. (11) as: a dropping of the 't Hooft term lifts the bottom of the effective potential  $\tilde{U}$  when the  $\tilde{\sigma}_x$  remains sizable and then leads to a smaller pressure. And after the chiral symmetry is restored, the  $\tilde{\sigma}_x$  is always nearly zero and the minimum of  $\tilde{U}$  would not be affected by the 't Hooft term.

Since pressure is crucial for the thermodynamics of the system, other thermodynamical quantities will all be

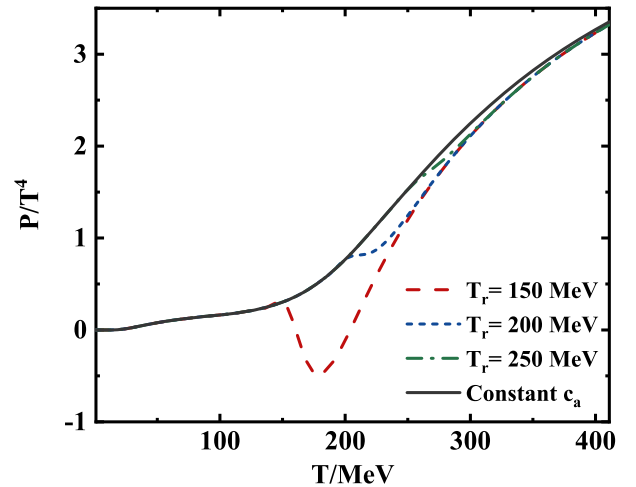


FIG. 9. Calculated normalized pressure as functions of temperature at several values of  $T_r$ .

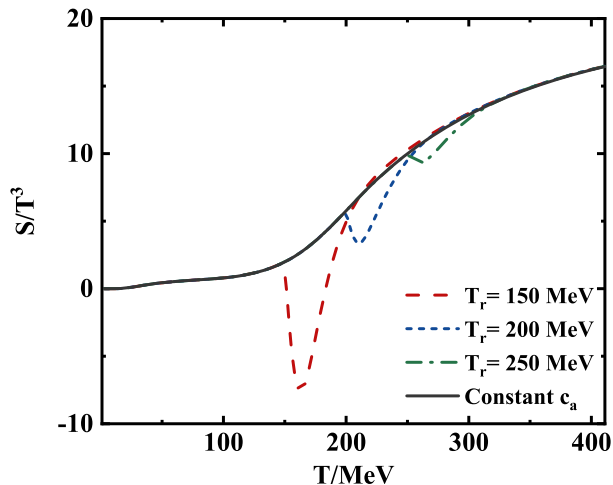


FIG. 10. Calculated normalized entropy density as functions of temperature at several values of  $T_r$ .

affected by it. For example, it can be seen in Fig. 10 that the entropy density, which is simply the derivative of pressure with respect to the temperature, gets also reduced and even becomes negative if the  $U_A(1)$  symmetry gets restored at a lower temperature. These unnatural behaviors of entropy will then affect the speed of sound  $c_s^2$  which is depicted in Fig. 11. We can see that  $c_s^2$  will oscillate and become negative if the  $U_A(1)$  symmetry gets restored too early; this is simply because of the negative entropy and specific heat at that temperature region. Even after the chiral phase transition happens, the  $U_A(1)$  restoration will continue to increase the  $c_s^2$  to exceed the ideal gas limit  $1/3$  until its restoration temperature is much higher than  $T_c^X$ .

We can observe from the above discussion that the contributions of the  $U_A(1)$  symmetry breaking embodied in the instanton background of QCD are crucial for the

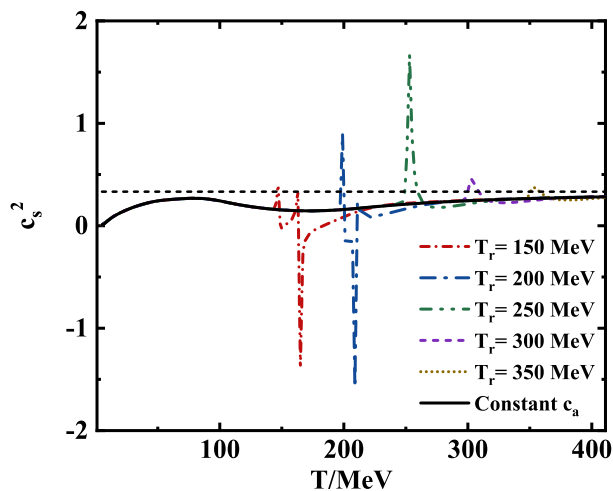


FIG. 11. Calculated speed of sound  $c_s^2$  as functions of temperature at several values of  $T_r$ . The short dashed black line denotes the ideal gas limit  $1/3$ .

thermodynamics of the system before the chiral phase transition (more exactly, crossover) is completed, then even a slight drop of the  $c_a$  will result in a unphysical pressure, entropy density, and speed of sound at that temperature region. After the chiral phase transition happens, the contributions of the instantons become ignorable, and then the  $U_A(1)$  symmetry can be restored gradually without causing any unphysical results. Thus, we speculate that the  $U_A(1)$  symmetry should be restored much later than the chiral symmetry  $SU_A(3)$  in order to obtain a physical pressure of the system.

#### IV. SUMMARY AND REMARKS

In this article, we investigate the effective restoration of the  $U_A(1)$  symmetry via the FRG approach combined with the  $2+1$  flavor PQM model. The 't Hooft term  $c_a \xi$  is parametrized as a function of temperature to imitate the  $U_A(1)$  symmetry restoration. Order parameters, meson spectrum, mixing angles, pressure, entropy density, and speed of sound of the system are calculated to explore the effects of  $U_A(1)$  restoration.

The calculated order parameters manifest that the chiral and deconfinement phase transition will be triggered at a lower temperature if the  $U_A(1)$  symmetry restoration happens too early, which agrees with the predictions given in Refs. [17,20,51]. The calculated meson spectrum shows that the  $(a_0, \pi)$  gets degenerate later than the  $(\sigma, \pi)$  multiplet and suggests a breaking of the  $U_A(1)$  symmetry as the chiral phase transition occurs, which is consistent with the lattice QCD simulation result [9]. Moreover, the mixing angle  $\theta_p$  of the  $\eta, \eta'$  system is shown to be highly sensitive to the  $U_A(1)$  restoration and can provide useful information about the status of  $U_A(1)$  symmetry.

Besides, we provide a new insight about the  $U_A(1)$  symmetry restoration problem: the system will have a negative and thus, unphysical pressure, entropy density, and speed of sound if the  $U_A(1)$  symmetry is restored before the chiral phase transition. These unphysical behaviors of the thermodynamical quantities can only be avoided if the  $U_A(1)$  symmetry keeps being broken until a temperature much higher than the  $T_c^X$  is reached.

Combining the results from meson spectrum and the thermodynamical properties, we speculate that the  $U_A(1)$  symmetry remains broken as the chiral symmetry  $SU_A(3)$  gets restored. And some underlying mechanisms are discussed. Moreover, we would like to mention that our work only considers the physical point in the Columbia plot (see also Ref. [35] for further investigations), while the  $U_A(1)$  symmetry breaking might have different fate in other region of the Columbia plot. For example, some lattice QCD simulations show that the  $U_A(1)$  symmetry is restored near the chiral phase transition in chiral limit with two flavor quarks [11,12]. Besides, as mentioned above, the  $\eta$ - $\eta'$  mixing problem also needs more comprehensive study. The related investigations in FRG approach are under progress.

## ACKNOWLEDGMENTS

The work was supported by the National Natural Science Foundation of China under Contracts No. 11435001, No. 11775041, and the National Key Basic Research Program of China under Contract No. 2015CB856900.

- 
- [1] G. 't Hooft, *Phys. Rev. Lett.* **37**, 8 (1976); *Phys. Rev. D* **14**, 3432 (1976).
- [2] E. Witten, *Nucl. Phys.* **B156**, 269 (1979).
- [3] D. J. Gross, R. D. Pisarski, and L. G. Yaffe, *Rev. Mod. Phys.* **53**, 43 (1981); R. D. Pisarski and L. G. Yaffe, *Phys. Lett.* **97B**, 110 (1980).
- [4] R. D. Pisarski and F. Wilczek, *Phys. Rev. D* **29**, 338 (1984).
- [5] F. R. Brown, F. P. Butler, H. Chen, N. H. Christ, Z. H. Dong, W. Schaffer, L. I. Unger, and A. Vaccarino, *Phys. Rev. Lett.* **65**, 2491 (1990).
- [6] T. Schäfer and E. V. Shuryak, *Rev. Mod. Phys.* **70**, 323 (1998).
- [7] D. E. Kharzeev, *Ann. Phys. (Amsterdam)* **325**, 205 (2010).
- [8] B. Alles, M. D'Elia, and A. Di Giacomo, *Nucl. Phys.* **B494**, 281 (1997).
- [9] T. Bhattacharya *et al.* (hotQCD Collaboration), *Phys. Rev. Lett.* **113**, 082001 (2014).
- [10] S. Aoki *et al.* (JLQCD and TWQCD Collaborations), *Phys. Lett. B* **665**, 294 (2008).
- [11] B. B. Brandt, A. Francis, H. B. Meyer, O. Philipsen, D. Robaina, and H. Wittig, *J. High Energy Phys.* **12** (2016) 158.
- [12] K. Suzuki (JLQCD Collaboration), *Proc. Sci., LATTICE2018* (**2018**) 152 [arXiv:1812.06621].
- [13] J. M. Pawłowski, *Phys. Rev. D* **58**, 045011 (1998).
- [14] S. Benic, D. Horvatic, D. Kekez, and D. Klabucar, *Phys. Rev. D* **84**, 016006 (2011); *Phys. Lett. B* **738**, 113 (2014).
- [15] R. Alkofer, C. S. Fischer, and R. Williams, *Eur. Phys. J. A* **38**, 53 (2008).
- [16] D. Horvatic, D. Kekez, and D. Klabucar, *Phys. Rev. D* **99**, 014007 (2019).
- [17] J. Schaffner-Bielich, *Phys. Rev. Lett.* **84**, 3261 (2000).
- [18] J. T. Lenaghan, D. H. Rischke, and J. Schaffner-Bielich, *Phys. Rev. D* **62**, 085008 (2000).
- [19] K. Fukushima, K. Ohnishi, and K. Ohta, *Phys. Rev. C* **63**, 045203 (2001).
- [20] P. Costa, M. C. Ruivo, C. A. de Sousa, and Y. L. Kalinovsky, *Phys. Rev. D* **70**, 116013 (2004); **71**, 116002 (2005).
- [21] B.-J. Schaefer and M. Wagner, *Phys. Rev. D* **79**, 014018 (2009).
- [22] H. Nagahiro and S. Hirenzaki, *Phys. Rev. Lett.* **94**, 232503 (2005).
- [23] H. Nagahiro, M. Takizawa, and S. Hirenzaki, *Phys. Rev. C* **74**, 045203 (2006).
- [24] W. J. Fu, Z. Zhang, and Y. X. Liu, *Phys. Rev. D* **77**, 014006 (2008).
- [25] M. Ciminale, R. Gatto, N. D. Ippolito, G. Nardulli, and M. Ruggieri, *Phys. Rev. D* **77**, 054023 (2008).
- [26] K. Fukushima, *Phys. Rev. D* **77**, 114028 (2008).
- [27] J. W. Chen, K. Fukushima, H. Kohyama, K. Ohnishi, and U. Raha, *Phys. Rev. D* **80**, 054012 (2009).
- [28] G. V. Dunne and A. Kovner, *Phys. Rev. D* **82**, 065014 (2010).
- [29] U. S. Gupta and V. K. Tiwari, *Phys. Rev. D* **81**, 054019 (2010).
- [30] Z. H. Guo, J. A. Oller, and J. R. de Elvira, *Phys. Lett. B* **712**, 407 (2012).
- [31] S. Sakai and D. Jido, *Phys. Rev. C* **88**, 064906 (2013).
- [32] A. G. Nicola and J. R. de Elvira, *J. High Energy Phys.* **03** (2016) 186; *Phys. Rev. D* **97**, 074016 (2018); **98**, 014020 (2018).
- [33] M. Mitter and B.-J. Schaefer, *Phys. Rev. D* **89**, 054027 (2014).
- [34] F. Rennecke and B.-J. Schaefer, *Phys. Rev. D* **96**, 016009 (2017).
- [35] S. Resch, F. Rennecke, and B.-J. Schaefer, *Phys. Rev. D* **99**, 076005 (2019).
- [36] C. Wetterich, *Phys. Lett. B* **301**, 90 (1993).
- [37] D. F. Litim, *Phys. Lett. B* **486**, 92 (2000).
- [38] D. F. Litim, *Phys. Rev. D* **64**, 105007 (2001).
- [39] D. F. Litim, *Phys. Lett. B* **393**, 103 (1997); *J. High Energy Phys.* **11** (2001) 059; *Int. J. Mod. Phys. A* **16**, 2081 (2001).
- [40] D. F. Litim and J. M. Pawłowski, *J. High Energy Phys.* **11** (2006) 026.
- [41] F. Freire and D. F. Litim, *Phys. Rev. D* **64**, 045014 (2001); D. F. Litim and D. Zappala, *Phys. Rev. D* **83**, 085009 (2011).
- [42] B. Stokić, B. Friman, and K. Redlich, *Eur. Phys. J. C* **67**, 425 (2010).
- [43] J. M. Pawłowski, *Ann. Phys. (Amsterdam)* **322**, 2831 (2007).
- [44] H. Gies, *Lect. Notes Phys.* **852**, 287 (2012).
- [45] W. J. Fu, J. M. Pawłowski, and F. Rennecke, arXiv:1909.02991.
- [46] T. K. Herbst, M. Mitter, J. M. Pawłowski, B.-J. Schaefer, and R. Stiele, *Phys. Lett. B* **731**, 248 (2014).
- [47] A. N. Tawfik and N. Magdy, *Phys. Rev. C* **90**, 015204 (2014).
- [48] W. J. Fu, J. M. Pawłowski, and F. Rennecke, arXiv:1808.00410; *Phys. Rev. D* **100**, 111501(R) (2019).
- [49] R. Wen, C. Huang, and W. J. Fu, *Phys. Rev. D* **99**, 094019 (2019); K. X. Sun, R. Wen, and W. J. Fu, *Phys. Rev. D* **98**, 074028 (2018); W. J. Fu, *Chin. Phys. C* **43**, 074101 (2019).
- [50] G. Fejos and A. Hosaka, *Phys. Rev. D* **94**, 036005 (2016).
- [51] S. K. Rai and V. K. Tiwari, arXiv:1812.06786.
- [52] K. Kamikado and T. Kanazawa, *J. High Energy Phys.* **01** (2015) 129.
- [53] X. Li, W. J. Fu, and Y. X. Liu, *Phys. Rev. D* **99**, 074029 (2019).

- [54] G. Fejos, *Phys. Rev. D* **92**, 036011 (2015); G. Fejos and A. Hosaka, *Phys. Rev. D* **95**, 116011 (2017); **98**, 036009 (2018).
- [55] Y. Jiang and P. F. Zhuang, *Phys. Rev. D* **86**, 105016 (2012); Y. Jiang, T. Xia, and P. F. Zhuang, *Phys. Rev. D* **93**, 074006 (2016); T. Xia, L. Y. He, and P. F. Zhuang, *Phys. Rev. D* **88**, 056013 (2013).
- [56] P. Kovács, Z. Szép, and G. Wolf, *Phys. Rev. D* **93**, 114014 (2016).
- [57] A. Bazavov *et al.* (hotQCD Collaboration), *Phys. Rev. D* **85**, 054503 (2012); *Phys. Rev. Lett.* **109**, 192302 (2012); *Phys. Rev. D* **90**, 094503 (2014).
- [58] S. Borsanyi, Z. Fodor, C. Hoelbling, S. D. Katz, S. Krieg, C. Ratti, and K. K. Szabo, *J. High Energy Phys.* **09** (2010) 073; S. Borsanyi, Z. Fodor, C. Hoelbling, S. D. Katz, S. Krieg, and K. K. Szabo, *Phys. Lett. B* **730**, 99 (2014).